DOI: 10.32615/ps.2019.166 PHOTOSYNTHETICA 58 (SI): 497-506, 2020

Special issue in honour of Prof. Reto J. Strasser

Analysis of OJIP transients during photoinactivation of photosystem II indicates the presence of multiple photosensitizers *in vivo* and *in vitro*

I. IERMAK[*,**,***], M. SZABÓ[#,##], and A. ZAVAFER[###]

Laboratory of Biophysics, Wageningen University, P.O. Box 8128, 6700 ET, Wageningen, The Netherlands[*]
BioSolar Cells Project Office, P.O. Box 98, 6700 AB, Wageningen, The Netherlands[**]
São Carlos Institute of Physics, University of São Paulo, São Carlos, SP, Brazil[***]
Institute of Plant Biology, Biological Research Centre, Hungarian Academy of Sciences, 6726 Szeged, Hungary[#]
Climate Change Cluster, University of Technology Sydney, Ultimo 2007, Australia[##]
Research School of Biology, College of Medicine, Biology and Environment, The Australian National University, Canberra ACT 2601, Australia[###]

Abstract

Generally, excessive excitation absorbed by the pigments is considered the cause of PSII photodamage. Previous studies of action spectra of PSII photodamage concluded that shorter wavelengths induce more damage, supporting the hypothesis of the existence of more than one photosensitizer. However, the relative influence of different photosensitizers is still inconclusive. In this work, we have revisited this question by inducing PSII photodamage *in vivo* and *in vitro* at two different wavelengths (460 and 660 nm) where the net absorption cross section was the same using equal irradiance. To correlate PSII photodamage with each wavelength band, we followed its time course using the OJIP transient of the chlorophyll fluorescence to determine the possible contributions of photoinhibition by different photosensitizers. We found evidence that at least two sites of photoinactivation of PSII exist.

Additional key words: absorptance; chlorophyll fluorescence; manganese cluster; photodamage; spinach; two-photon excitation microscopy.

Introduction

Plants depend on light to survive but light absorption has the side effect of photodamage to the photosynthetic machinery (van Gorkom and Schelvis 1993). Photodamage correlates directly with the light irradiance, which means that even at low irradiances there is still some degree of photodamage (Tyystjärvi and Aro 1996, Oguchi *et al.* 2011a,b; 2013). For example, Tyystjärvi and Aro (1996) demonstrated that the rate of photoinhibition at 100 μmol(photon) m^{-2} s^{-1} is 10% of the rate of photoinhibition at 1,000 μmol(photon) m^{-2} s^{-1}.

While the exact mechanism of PSII photodamage is far from established, there is a consensus (Melis 1999, Nishiyama *et al.* 2006, Murata *et al.* 2007, Takahashi and Murata 2008, Oguchi *et al.* 2011b, Vass 2011, 2012; Schreiber and Klughammer 2013, Tyystjärvi 2013) that: (*1*) the most affected component of photosynthesis is PSII (Ohad *et al.* 1990, Aro *et al.* 1993); (*2*) the photodamage rate (usually expressed as the rate coefficient k_{PI}) is directly proportional to irradiance (Tyystjärvi and Aro 1996); (*3*) UV wavelengths induce preferential damage to the Mn_4O_5Ca cluster of PSII (Hakala *et al.* 2005); (*4*) the quantum efficiency of photodamage is higher at shorter wavelengths (Zavafer *et al.* 2015a); and (*5*) after the initial event of photodamage (inactivation of the PSII), the subunit D1 has to be degraded and a new D1 synthesized in order to recover photosynthetic activity (Ohad *et al.* 1990, Aro *et al.* 1993).

Available hypotheses can be classified based on photo-

Received 28 August 2019, *accepted* 6 December 2019.
+Corresponding author; e-mail: alonso.zavaleta@anu.edu.au
Abbreviations: Chl – chlorophyll; HWHM – half width half maximum; LED – light-emitting diodes; NPQ – nonphotochemical quenching; ROS – reactive oxygen species; UV-Vis – ultraviolet and visible.
Acknowledgements: This research was financed in part by the BioSolar Cells open innovation consortium, supported by the Dutch Ministry of Economic Affairs, Agriculture and Innovation (I. Iermak). A. Zavafer acknowledges Australian Research Council (Discovery grant DP120100872). A. Zavafer is grateful to his PhD sponsors National Council of Science and Technology of Mexico (CONACYT) and the Mexican Secretariat of Public Education (SEP). A.Zavafer and I. Iermak are grateful to Mr. John Philippi for all the technical help during the development of this project and to Prof. Reto J. Strasser for providing an *M-PEA* fluorometer. A. Zavafer thanks Prof. Shunichi Takahashi for supplying the LED boxes. M. Szabó acknowledges funding from the Hungarian Academy of Sciences (PREMIUM-2017-38) and The National Research, Development and Innovation Office (NKFI FK 128977). The authors would like to thank Prof. Eldon Ball for help in improving this work.

sensitizers into three groups to explain PSII photodamage. The hypothesis of light energy absorbed by photosynthetic pigments (which includes the excessively absorbed energy hypothesis) proposes that light absorbed by chlorophylls (Chl) induces accumulation of reactive oxygen species (ROS), in particular, singlet oxygen.

The two-step hypothesis (also referred as direct damage of the Mn_4O_5Ca cluster) states that photodamage primarily affects the Mn_4O_5Ca cluster because of direct absorption of light (Hakala *et al.* 2005, Ohnishi *et al.* 2005). It has been proposed that light absorption induces breakdown and inactivation of the Mn_4CaO_5 cluster (Hakala *et al.* 2005). For this reason, some authors have proposed that PSII photodamage is independent of excessive excitation (Tyystjärvi and Aro 1996, Melis 1999, Nishiyama *et al.* 2006, 2007; Murata *et al.* 2007, Takahashi and Murata 2008, Tyystjärvi 2008, Takahashi *et al.* 2010, Takahashi and Badger 2011, Campbell and Tyystjärvi 2012, Tyystjärvi 2013, Nishiyama and Murata 2014).

A more recent hypothesis, the hybrid hypothesis, states that both mechanisms (light energy absorbed by photosynthetic pigments and the Mn hypothesis) occur in parallel (Oguchi *et al.* 2011b, 2013; Schreiber and Klughammer 2013). Each mechanism, to a different extent, could be dependent on wavelength (Oguchi *et al.* 2011b, Schreiber and Klughammer 2013), experimental material (Oguchi *et al.* 2011b, 2013; Schreiber and Klughammer 2013), and depth in the tissue (Oguchi *et al.* 2011b, 2013).

In an attempt to resolve the controversy over the mechanisms and explanations of PSII photodamage, in this study, we examined the wavelength dependency of PSII photodamage *in vivo* and *in vitro*. For this purpose, we photodamaged samples *in vivo* and *in vitro* using the same irradiance at two different wavelengths that have nearly the same integrated absorption cross section (*see* 'Experiment rationale' for a definition). By comparing the photosynthetic response using OJIP curves, two-photon microscopy and reflectance spectroscopy, the wavelength-dependent role of the photosensitizers was evaluated.

Materials and methods

Experiment rationale: In this work, we compared the kinetic changes of the OJIP transients during photodamage of PSII in the absence of repair. The two wavelengths selected for this work have the same probability of absorption (absorption cross section) for PSII-enriched membranes (Fig. 1*A*,*B*), implying that the excitation at those wavelengths is the same and therefore electron transport rates are expected to be similar between the two. In case that two or more photosensitizers cause PSII photoinactivation, different rates of changes in the OJIP trends are to be expected at different wavelengths. As the different phases of the OJIP curve reflect the performance of various sections of the light reactions, changes in the OJIP phases at separate wavelengths would indicate the effect of photoinhibition on distinct components of photosynthesis. Finally, the comparison between PSII particles (*in vitro*) and leaves (*in vivo*) has the objective of illustrating the effect of light penetration depth (absent *in vitro*) during the experimental time course and the effect of the pool of electron acceptors (which is only present *in vivo*). Both systems are in excessive excitation conditions, moreover, in PSII-enriched membranes, the functional electron acceptor pool is absent and leaves illuminated at low temperature have a lower rate of electron transport *in vivo* (Hendrickson *et al.* 2004) and some components of NPQ are arrested or operate at a very low rate (Verhoeven 2014). Also, it should be noted that PSII-enriched membranes were selected as an *in vitro* model because photodamage was studied using similar wavelength to investigate the causes of photodamage induction by Zavafer *et al.* (2015b, 2017). Based on these arguments, the two experimental model systems can be considered comparable.

Plant material and sample preparation: Fresh and intact spinach leaves were purchased at local markets (Wageningen, NL). The leaves were stored at 4°C in a cold room with the petiole submerged in tap water until use. Plants with high F_V/F_M values (0.82 to 0.78) were selected for all experiments.

PSII-enriched membranes were prepared from fresh market spinach as described by Berthold *et al.* (1981). Then the sample was solubilized in standard buffer (400 mM sucrose, 25 mM MES-NaOH, 15 mM NaCl, 5 mM $MgCl_2$, pH 6.5) and aliquots were flash-frozen in liquid nitrogen and stored at −80°C until use. Before light exposure, the sample was thawed and resuspended in the standard buffer without sucrose (salt buffer). Then it was centrifuged at 16,000 × *g* for 5 min to remove any traces of sucrose and the pellet was resuspended again in a salt buffer. The Chl content was measured according to Porra *et al.* (1989) and adjusted to 150 μg(Chl) mL^{-1} (this is further referred to as PSII-enriched membrane stock solution). The sample was kept in darkness at 4°C at all times unless otherwise stated.

Photodamage experiments: In order to compare the effect of photodamage on PSII, light exposures *in vivo* and *in vitro* were done at the same temperature (4°C) using the same light source. All experiments were done at 4°C because this is the temperature where PSII-enriched membranes are stable.

For photodamage experiments performed *in vivo*, PSII repair in leaves was inhibited by uptake of 5 mM lincomycin through the petiole for 12 h at 4°C at low light intensity [< 5 μmol(photon) m^{-2} s^{-1}] (Oguchi *et al.* 2009, 2011b; Matsubara and Chow 2004). Leaves were transferred to plastic Petri dishes containing a layer of water of 1 mm to ensure moistening (Fig. 1S, *supplement*). The adaxial side of each leaf faced the light. Then the Petri dishes were placed inside custom-made LED light boxes (photoinhibition boxes) made of aluminium (Fig. 1S*A*,*D*). The irradiance at the surface of the leaf upon illumination was 1,300 μmol(photon) m^{-2} s^{-1} of monochromatic light (λ_{peak} = 460 ± 10 nm or λ_{peak} = 660 ± 10 nm, peak profile for each LED can be found in Zavafer *et al*. 2017). This intensity was selected because the electron transport rates as a function of irradiance deviate from a linear relation above 200 μmol(photon) m^{-2} s^{-1} in spinach leaves (Evans and Terashima 1987). It is therefore assumed that leaves

were under excessive energy absorption. To ensure that the amount of excessive excitation was the same at the same irradiance, light of wavelengths of 460 and 660 nm was chosen for this study. Fig. 1*A* shows that the net absorption for both wavelengths is the same, as the area under the spectrum is the same for both LED sources. The area was calculated by integrating the region under the absorption spectrum in the interval defined by [$\lambda_{peak} - 0.5 \times$ (HWHM), $\lambda_{peak} + 0.5 \times$ (HWHM)] where HWHM refers to the 50% width half maximum of the peak of each LED [based on Zavafer *et al.* (2015b)]. In this manner, the only difference between the two light sources is the wavelength. The samples were illuminated for 30, 60, 120, 180, and 300 min. The control group was kept under identical conditions in darkness inside the photoinhibition boxes. The light was provided by 16 LEDs of 3 W each bolted into the lid of the aluminium boxes (Fig. 1S*A*,*D*). To suppress the heat from the LED array, the box lid was attached to a cooling block (Fig. 1S*B*,*D*). Water at 4°C passed through the cooling block, and in this way not only was the heat removed but also stability of the LED sources was ensured (Fig. 1S*F*). The temperature of the box lid was 6°C at the plate and 12°C at the LED. The sample was kept floating in contact with 4°C water inside the box (Fig. 1S*H*).

All sample handling for PSII-enriched membranes was done at 4°C. The PSII-enriched membrane solution was adjusted to a total concentration of Chl (*a*+*b*) of 150 μg mL^{-1} diluted in standard buffer. Then the sample was transferred to sterile plastic Petri dishes. The optical path length was 2.5 mm (to compensate the applied high Chl concentration with a very thin path length). To ensure that the volume remained the same during the whole illumination period, Petri dishes were closed and sealed with parafilm. Each Petri dish was transferred to the LED photoinhibition boxes. The Petri dish was kept in contact with water at 4°C. The irradiance at the surface of the liquid was 1,300 μmol(photon) m^{-2} s^{-1}. Samples were illuminated with either 460 or 660 nm light for 1, 2.5, 5, 20, and 60 min (shorter illumination was used because PSII-enriched membranes were completely inactivated after 1 h of illumination). Because PSII-enriched membranes were illuminated in the absence of any artificial electron acceptor, the system was under excessive excitation. To ensure that the irradiance and amount of excessive excitation were the same, 460 and 660 nm LED light was chosen for this study because the spectral profile of both light sources has the same net absorption by photosynthetic pigments (Fig. 1*D*). In this manner, the only difference between the two light sources was the wavelength. PSII-enriched membranes were centrifuged at 20,000 × *g* to remove the salt buffer, then the pellet was resuspended in a standard buffer (sucrose rich) for cryogenic storage. The sample was frozen in liquid nitrogen and stored at −80°C until use.

Polyphasic Chl *a* fluorescence rise measurements: The Petri dishes, which contained the leaves, were removed from the light, and dark-adapted for at least 1 h at room temperature to ensure any quenching mechanisms were relaxed. Chl fluorescence was measured from petiole to tip for every leaf in three different regions to cover as large leaf area as possible. After the measurements were finished, the leaves were transferred back to the LED photoinhibition boxes to continue with the photodamage experiment. This process was repeated for every time point until the experiment was finished. The continuous rise of the Chl *a* fluorescence was measured at room temperature (in a temperature-controlled room at 25°C) using a *Multichannel-Plant Efficiency Analyzer 2* (*M-PEA*, *Hansatech Instruments*, UK) (for a full description of the instrument *see* Strasser *et al.* 2010). The actinic light was 660 nm with an intensity of 3,000 μmol(photon) m^{-2} s^{-1} for 10 s. All sample manipulation occurred under green light of less than 1 μmol(photon) m^{-2} s^{-1} irradiance.

For measuring the PSII activity of PSII-enriched membranes, the photodamaged sample was defrosted at 4°C and then diluted with standard buffer and centrifuged at 20,000 × *g*. This was done primarily to ensure the PSII-enriched membranes were in optimum condition. Then the concentration of the PSII-enriched membranes was readjusted to 150 μg(Chl) mL^{-1}. PSII activity was assayed by measuring Chl *a* fluorescence in the same way as described above. The sample of 30 μL was transferred to a piece of wet filter paper before measurement. All sample manipulation occurred under green light with an intensity of 1 μmol(photon) m^{-2} s^{-1} or in complete darkness.

Two-photon excitation microscopy: The OJIP method assumes that the F_O approximates to the value of the fluorescence at 20 μs after the onset of actinic light; however, in leaves, most of the measured fluorescence comes from the upper layers of the photosynthetic tissue. It is known that PSII photodamage at different wavelengths is affected by the penetration of light. This means potential artefacts could be observed in the OJIP assessment if one cannot measure across the depth of tissue. In order to have an independent assessment of F_O, we used two-photon excitation microscopy to assess F_O in the upper layer of the tissue exclusively. Imaging was performed in a multiphoton *Biorad Radiance 2100 MP* system, coupled to a *Nikon TE300* inverted microscope (Laptenok *et al.* 2010). A tuneable *Ti-Sapphire* laser *Coherent Mira* was used as an excitation source. It was pumped with a 5 W *Coherent Verdi* laser. Excitation pulses of 860 nm were 250 fs long and a repetition rate of 76 MHz was used. A *Nikon 60 x* water immersion apochromat objective (*NA 1.2*) focused the laser beam. The fluorescence was detected by non-descanned direct detectors *via* a *Hamamatsu R3809U* photomultiplier, operated at 3.1 kV. Fluorescence was selected using a 680/13 nm interference filter and a 770 nm cut-off filter was used to prevent detection of the excitation beam. A neutral density filter was used in the excitation pass to reduce the excitation light intensity. The output of the detector was coupled to a *Becker & Hickl* single-photon counting module (*SPC 830*) (Becker and Bergmann 2003). The fluorescence was recorded for 5 min at a count rate of 10,000 counts per second.

Absorption spectroscopy: Absorption spectra were measured using a *Cary 4000 UV-Vis* spectrophotometer with

integrating sphere (*Agilent*, CA, USA). Liquid samples were measured in a quartz cuvette and the sample was placed inside of an integrating sphere. For leaves, the samples were measured in a diffuse reflectance configuration. Spectra were acquired with a 1-nm resolution from 350 to 850 nm. As the signal to noise ratio was poor below 350 and above 800 nm; these regions of the spectra were excluded.

Statistical analysis: Prompt fluorescence data (OJIP curves) were statistically processed using *OriginPro9.1* software or *Microsoft Excel 2013*. All observed kinetics were fitted to the following equation:

$$y_t = A_0 e^{(-k_{PI} \times t)} + y_0$$

where y_t is the value of a signal or parameter at a given time t, t is the time in h (*in vivo*) or min (*in vitro*), A_0 is the activity before illumination, k_{PI} is the rate constant and y_0 is the residual of the signal or parameter. This equation is used to estimate the k_{PI} or constant of photoinhibition, which allows determination of the effectiveness of inhibition for a given photosynthetic parameter. All digital processing of images was done using *Image J*.

Results

PSII activity decays in a single-exponential manner *in vitro* and *in vivo*: PSII activity was measured as the relative fraction of functional PSII ($1/F_O - 1/F_M$) (Havaux *et al.* 1991) upon illumination at 1,300 µmol(photon) m^{-2} s^{-1} in spinach leaves and PSII-enriched membrane particles (Fig. 1). The relative fraction of functional PSII was chosen as an indicator of PSII activity as it is directly proportional to the oxygen yield per single-turnover saturating flash (Matsubara and Chow 2004). It is widely accepted that during PSII photodamage, the PSII activity decays in a single-exponential manner (Vavilin *et al.* 1995, Campbell and Tyystjärvi 2012). We also observed that the relative fraction of functional PSII decreased (Fig. 1) in a

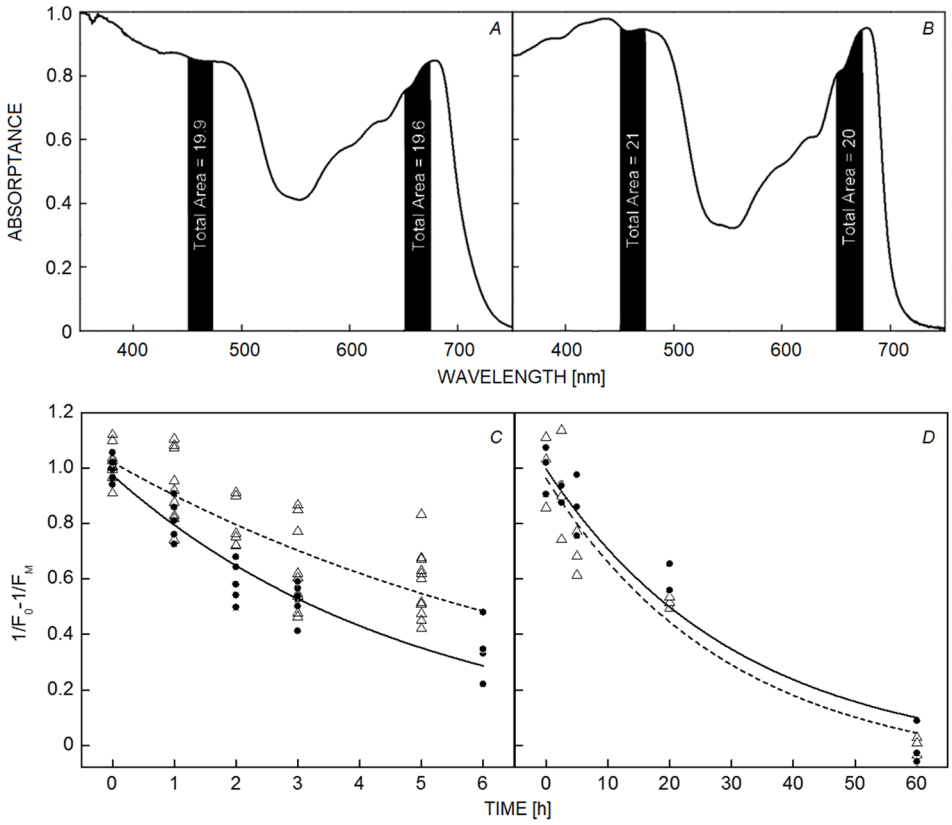

Fig. 1. Time course of PSII photodamage estimated as the relative fraction of functional PSII ($1/F_O - 1/F_M$). Samples illuminated with 1,300 µmol(photon) m^{-2} s^{-1} of 460 nm in *dark circles* and 660 nm in *white triangles*. (*A*) Absorptance spectrum of leaves (average of several samples), (*B*) absorptance spectrum of PSII-enriched particles. The relative fraction of absorbed light was calculated based on the total area calculated by integrating the area under the curve of the full width half maximum (FWHM) of 460 nm and 660 nm of each LED emission spectrum. (*C*) Spinach leaves, (*D*) PSII-enriched membranes. Leaves and PSII-enriched membranes were exposed to light at 4°C. Data points correspond to individual measurements and values of $1/F_O - 1/F_M$ have been normalized to the first time point. *In vivo* data originate from a representative data set of one of the two experiments, each time point was assessed from 2–3 leaves, each point represents the value of a measurement spot and each leaf was measured in at least two sites. Note that each time point consisted in measurements of a group of leaves. *In vitro* results originate from a representative data set of one of the two experiments where a single Petri dish was exposed. As in the *in vivo* measurements, each time point originates from an independent sample. Three aliquots were measured from each Petri dish. Spectral data correspond to the average of three leaves or three cuvettes with PSII-enriched membranes.

single-exponential manner (double exponential fitting was also attempted but the χ^2 and r^2 were < 0.95). In leaves, the magnitude of photodamage was greater at 460 nm than that at 660 nm (k_{460} = 0.21 ± 0.02 h^{-1} and k_{660} = 0.12 ± 0.01 h^{-1}) (Fig. 1*C*). By contrast, in PSII-enriched membranes, there was no clear difference between the two wavelengths (k_{460} = 0.03 ± 0.01 min^{-1} and k_{660} = 0.03 ± 0.01 min^{-1}) (Fig. 1*D*). This indicates that the wavelength dependency could be observed only *in vivo*.

Photodamage induces different changes to the prompt fluorescence transients *in vitro* and *in vivo*: In all conditions, the fluorescence intensity decreased as the photodamage advanced. In the case of leaves illuminated with 460 nm (Fig. 2S*A*, *supplement*) or 660 nm light (Fig. 2S*B*), the shape of the OJIP transient changed as photodamage advanced. In Fig. 2, one can see that all phases of the OJIP transient decreased in amplitude, but primarily the JI phase was affected (especially after 3 h, Fig. 2*B*).

PSII-enriched membranes presented a different change in the shape of the OJIP trend (Fig. 3*A*). The transients observed for PSII-enriched membranes (Fig. 2S*C*,*D*) showed a biphasic curve in which the J-step appeared at 5 ms (here on address as J') and the I-step was absent. The JI phase was practically absent and replaced with a plateau between 2 to 5 ms (denoted here as D). After F_M was reached (P-step), the fluorescence intensity declined in a similar manner as in leaves. The effect of photodamage on the prompt fluorescence transients in PSII-enriched membranes affected primarily its net intensity but not the shape of the curve. Also, light treatment at both wavelengths quenched the fluorescence to similar extents.

Table 1. T_{50} (the time required to induce 50% decrease in the amplitude of each phase of the OJIP curve) values for the decrease of OJ, JI, and IP phases after 460 and 660 nm illumination in leaves. Data are presented in h ± standard error.

	T_{50} [h]	
	460 nm	660 nm
OJ	0.62 ± 0.06	1.16 ± 0.17
JI	0.39 ± 0.06	0.66 ± 0.07
IP	1.05 ± 0.17	1.54 ± 0.27

The JI phase is the most affected *in vivo*: Individual OJIP phases are compared in Fig. 2, where each phase (OJ, JI, and IP) is normalized to the respective value at 0 h of illumination. Each phase presented a single-exponential decay (with a residual term and both illumination wavelengths were fitted by a global analysis using an empirical equation), and at 460 nm the decrease was faster than that at 660 nm (T_{50} values are presented in Table 1), in agreement with the data presented in Fig. 1. These data suggest that the JI phase was the most affected by photodamage, followed by the OJ phase, while the IP phase was the least affected.

***In vitro*, the two phases of the Kautsky induction curve decay similarly**: In order to explain the photodamage-induced changes in the *in vitro* system, the differences in the shape of the prompt fluorescence transients between the two model systems have to be described. To illustrate this further, the arithmetical difference between the two curves (*in vivo* and *in vitro*) was calculated (Fig. 3*A*). Positive bands in the difference curve indicated that the phase was absent in leaves (J'-step) and the negative bands indicated that it was absent in PSII-enriched membranes (I-, G-steps).

For PSII-enriched membranes, it was observed that the OJ' and J'P phases decreased by the same magnitude at both wavelengths and that the shape of the curve did not change throughout the treatment (Fig. 3*B*). This means that only the total rise of the prompt fluorescence, *i.e.*, variable fluorescence (F_V; *see* Fig. 3S, *supplement*), changed. The decrease in F_V followed a single-exponential decay and the rate of decay was not statistically different for both conditions (k_{460} = 0.07 ± 0.02 min^{-1} and k_{660} = 0.07 ± 0.01 min^{-1}) (Fig. 3S).

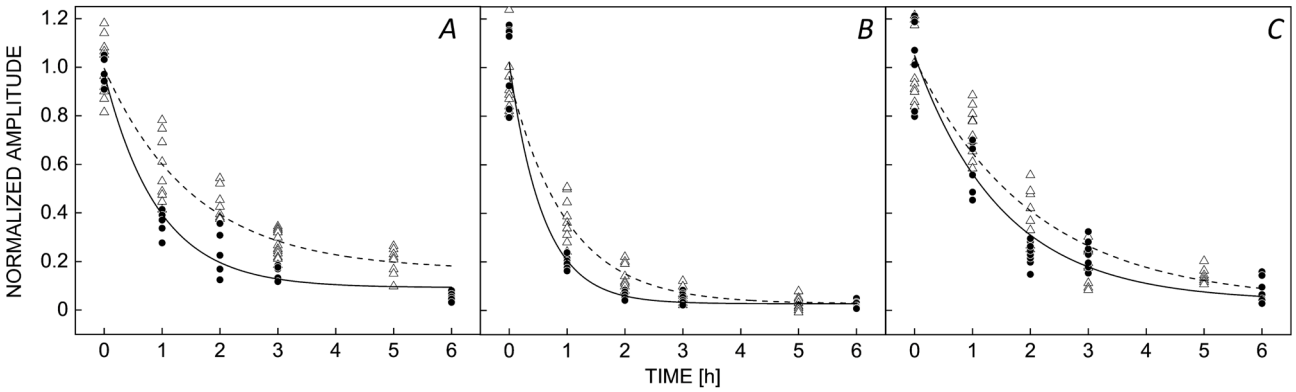

Fig. 2. Effect on the normalized amplitude of the individual phases of the OJIP curve due to PSII photodamage in leaves. Amplitudes of (*A*) OJ, (*B*) JI, and (*C*) IP were normalized to the respective values at 0 h. Samples were illuminated under the same conditions as Fig. 1 with 460 nm (blue) and 660 nm (red). *In vivo* data originate from a representative data set of one of the two experiments, each time point was assessed from 2–3 leaves, each point represents a measurement and each leaf was measured in at least two sites. Note that each group of leaves for every time point was different.

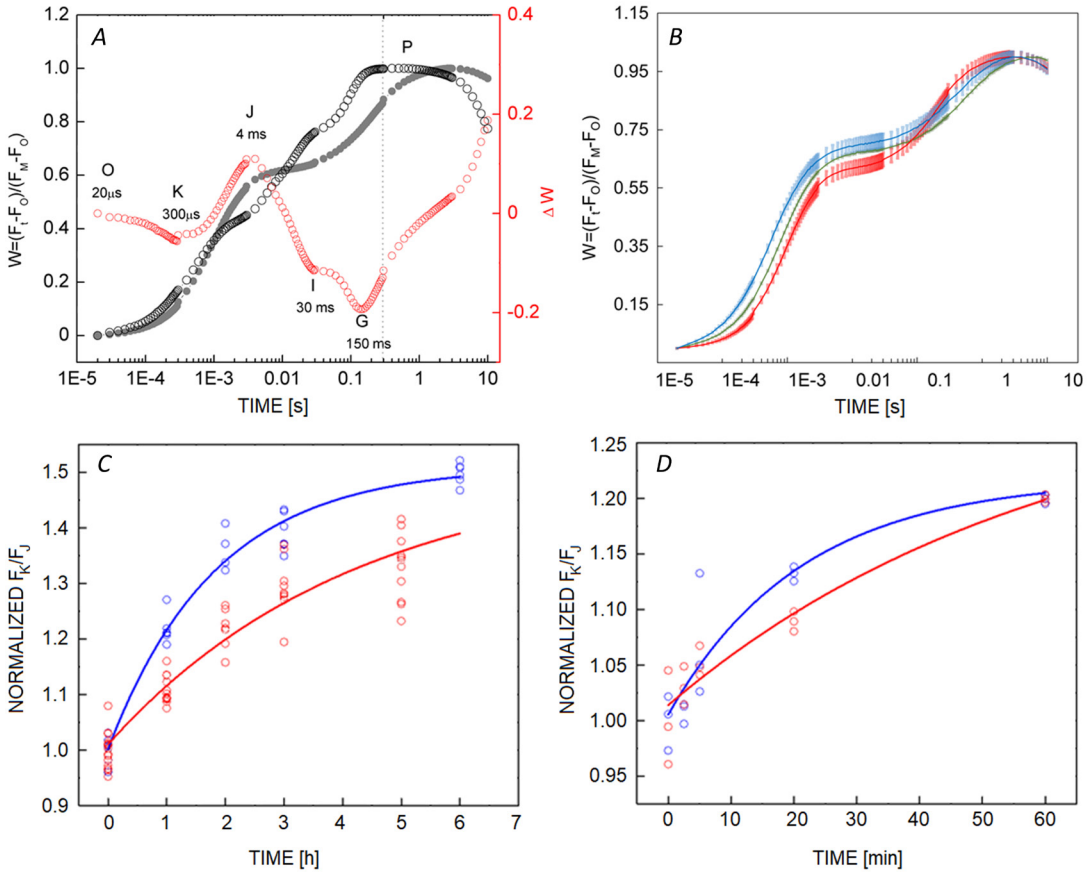

Fig. 3. Effect of photodamage of PSII on the shape of the OJIP curve in leaves and PSII-enriched membranes. (*A*) Leaves (*black open circles*) and PSII-enriched membranes (*grey closed circles*) were compared by calculating $W = (F_t - F_O)/(F_M - F_O)$; in order to clarify the difference between the two curves, *in red* is presented $\Delta W = W_{Leaves} - W_{PSII\text{-}enriched\ membranes}$, which shows the difference in the prompt fluorescence steps between *in vivo* and *in vitro* model systems. The fluorescence transients are expressed as $(F_t - F_O)/(F_M - F_O)$ after 6 h of illumination with 460 nm (*blue*) and after 5 h of illumination with 660 nm (*red*) compared to the nonilluminated sample or 0 h illumination (*green*). (*B*) Photodamage-induced formation of the K-step in samples exposed to wavelengths of 460 (*blue*) and 660 nm (*red*) of light expressed as the ratio F_K/F_J for: (*C*) spinach leaves, (*D*) PSII-enriched membranes. *In vivo* data originate from a representative data set of one of the two experiments, each time point was assessed from 2–3 leaves, each point represents a measurement and each leaf was measured in at least two sites. Note that each time point was assessed from a group of leaves. *In vitro* results originate from a representative data set of one of the two experiments where a single Petri dish was exposed. In the same fashion to the *in vivo* measurements, each time point originates from an independent sample. Three aliquots where measured from each Petri dish. Spectral data correspond to the average of three leaves or three PSII-enriched cuvettes. OJIP curves correspond to average curves of control samples (leaves or PSII-enriched membranes).

Increase in the K-step reflects impairment of the OEC at both wavelengths: In some types of stress, a positive band appears at 300 µs, termed as the K-step, which is usually hidden in the OJIP curve, which reflects impairments to the Mn_4O_5Ca functionality (Srivastava *et al.* 1997, Strasser 1997, Tóth *et al.* 2011). If the value of fluorescence at 300 µs ($F_{300\mu s}$) is normalized to the value of the J-step ($F_{300\mu s}/F_J$), it is possible to determine by how much the K-step increased. The results of these calculations are presented in Fig. 3*C*,*D*. We can observe that for both wavelengths there was an increase in the formation of the K-step in a single-exponential fashion. In leaves, 460 nm light (Fig. 3*C*) induced a faster increase of the K-step in comparison with 660 nm light ($k_{460} = 0.59 \pm 0.07\ h^{-1}$ and $k_{660} = 0.26 \pm 0.02\ h^{-1}$). In a similar fashion, in PSII-enriched membranes (Fig. 3*D*), the increase in the K-step followed single-exponential kinetics, and this increase was faster at 460 nm than that at 660 nm ($k_{460} = 0.05 \pm 0.01\ min^{-1}$ and $k_{660} = 0.02 \pm 0.01\ min^{-1}$). This would mean that in both model systems the functionality of the Mn_4O_5Ca cluster was impaired in a wavelength-dependent manner.

Photobleaching is enhanced at 460 nm: We observed that at the latest time points of the experiment, leaves exposed to 460 nm light exhibited bleaching. If photobleaching occurs in parallel to photoinactivation *in vivo*, this would induce artefacts in the Chl fluorescence measurements, as the absorption cross section analyzed would be different at different wavelengths and time points. To determine the magnitude of photobleaching, we recorded the absorptance spectra of leaves at different time points (0, 1, 3, and 15 h)

of treatment (Fig. 4). As can be seen from the spectra (Fig. 4*A*), slight bleaching of pigments occurred after 3 h of blue light illumination (a decrease in 4% of the absorption), but a large decrease of absorption was observed after 15 h of treatment. In the case of illumination with red light (660 nm; Fig. 4*B*), no bleaching was observed after 3 h of treatment, and the extent of bleaching after 15 h of illumination was smaller than in the case of 460 nm light.

The effect of photodamage on F_O: As demonstrated in the previous section, we observed photodamage accompanied by photobleaching. Loss of photosynthetic pigments would lower the Chl content and also the fluorescence intensity. This would manifest itself as a decrease in the F_O values observed with the *M-PEA* fluorometer. As these phenomena could potentially induce artefacts in the interpretation of the results, we examined the effect of photodamage over the upper photosynthetic tissue layer using two-photon microscopy. Two-photon microscopy uses a NIR excitation (860 nm) to induce fluorescence, as the probability of this event is low, a two-photon excitation has negligible actinic effect. In other words, reaction centres remained open and the observed fluorescence value equaled F_O (Fig. 5). Fluorescence intensity decreased with time in both experimental conditions, however, 460 nm light had a stronger effect than that of 660 nm light. The same effect can be observed from the fluorescence images (Fig. 5*B–G*). When further measurements were done after 15 h of illumination, we observed that fluorescence completely disappeared after illumination with 460 nm light, and was severely quenched after illumination with 660 nm light.

Discussion

In the present work, a two-level comparison of photodamage was done between experimental model systems and light wavelength. In the first instance, the two experimental model systems were studied to identify similarities and differences between PSII photodamage *in vivo* and *in vitro* under equal photodamaging irradiance with the same absorption cross section. Then, we compared the wavelength-specific responses of the two systems, as it is hypothesized that the photosenzitizer-dependent

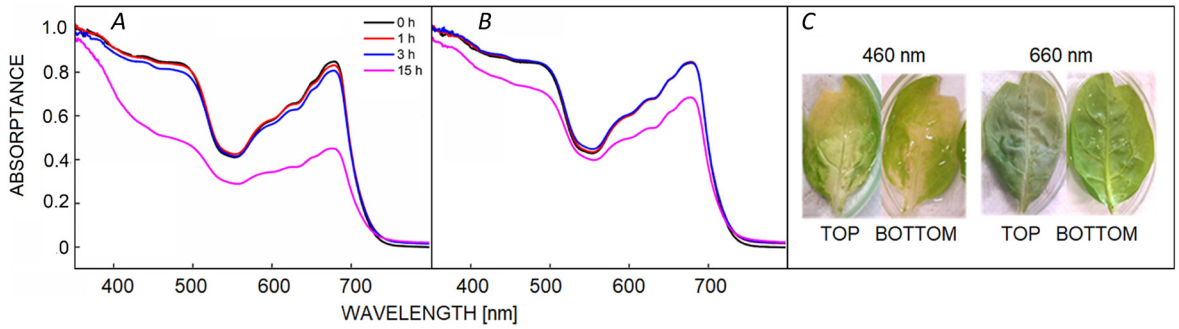

Fig. 4. Absorptance spectra of spinach leaves, recorded after 0, 1, 3, and 15 h of illumination with (*A*) blue light (460 nm), (*B*) red light (660 nm). Spectra were normalized to the value of a control leaf (0 h) at 350 nm. (*C*) Adaxial (*top*) and abaxial (*bottom*) sides of the spinach leaf after 15 h of illumination. *In vivo* data originates from a representative data set of one of the two experiments, each time point was assessed from 2–3 leaves. Spectral data correspond to the average of three leaves measured at the central part of leaf lamina.

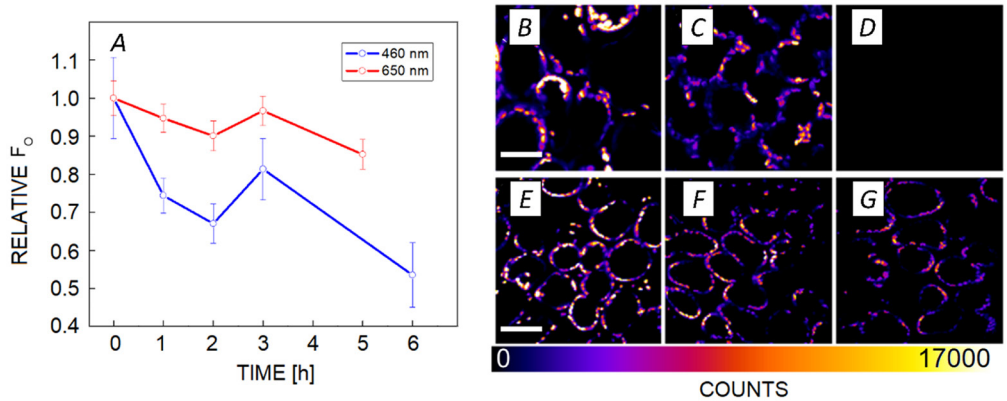

Fig. 5. Effect of photodamage on F_O in leaves probed by two-photon microscopy. (*A*) Normalized fluorescence intensity during the time course of photodamage, obtained during illumination with 460 and 660 nm light; (*B–D*) fluorescence intensity-based images of spinach leaves for 460 nm at 0 (*B*), 6 (*C*), and 15 (*D*) h; scale bar = 21 μm. (*E–G*) Fluorescence intensity-based images of spinach leaves for 660 nm at 0 (*E*), 5 (*F*), and 17 (*G*) h; scale bar = 31.5 μm. Spinach chloroplasts were excited *via* two-photon absorption at 860 nm and detected with a bandpass filter centered at 680 nm and with a bandwidth of 13 nm. *In vivo* data originate from a representative data set of one of the two experiments, each time point was assessed from 2–3 leaves that yielded more than three micrographs.

mechanisms of photodamage are wavelength dependent. The behaviour of photodamage *in vivo* and *in vitro* has been a matter of discussion and has led authors to argue that the different mechanisms observed are a result of different experimental approaches (Melis 1999, Nishiyama *et al.* 2006, Murata *et al.* 2007, Takahashi and Murata 2008, Oguchi *et al.* 2011b, Vass 2011, 2012; Schreiber and Klughammer 2013, Tyystjärvi 2013). A key feature during PSII photodamage is the loss of functionality, which follows first-order kinetics (Campbell and Tyystjärvi 2012). We found in the current study that the decay in OJIP parameters follows first-order kinetics for both systems. Furthermore, in both model systems, a single-exponential kinetics was observed in the intensity of the K-step (suggesting impairment in the Mn cluster activity). The single-exponential kinetics observed in both systems and the presence of a K-step indicate that the mechanism of PSII photodamage is similar *in vivo* and *in vitro* under the described experimental conditions.

On the other hand, we observed some differences between *in vivo* and *in vitro* experiments. In PSII-enriched membranes, the photodamage at 460 and 660 nm showed no statistical difference. Our *in vitro* model lacks electron transport beyond Q_B and also its electron acceptor pool is quite small, so at the current conditions PSII-enriched membranes are under excessive excitation. In addition, the liquid sample was continuously stirred and this would remove any influence of differential light penetration of photoinhibition by different wavelengths (Zavafer *et al.* 2015b). In consequence, we observed that in PSII-enriched membranes, the total intensity of the OJIP curve decreased with equal magnitude, as excitation was the same in both samples. Since no wavelength dependence was observed, photodamage in our *in vitro* model cannot be explained by light absorption of the Mn cluster. Therefore, one has to assume that PSII photodamage would be governed by the photosensitizers related to excitation pressure such as photosynthetic pigments. One should note that the observed results do not support previous hypotheses that explain photodamage *in vitro* by direct light absorption by the Mn cluster (Zavafer *et al.* 2015b). In turn, the results presented here are more in agreement with the mechanism proposed by Zavafer *et al.* (2017) according to which photoinduced ROS are the agents that disrupt the Mn cluster.

In our experiment with leaves, allocation of the photo-damaging effect to individual photosensitizers is not possible. This is because PSII photodamage is modulated by differences in the penetration of light of different wavelengths in photosynthetic tissues, the presence of some NPQ mechanisms, and the presence of a larger electron transport pool. Therefore, our results based on the OJIP curve are explained better under the framework of the hybrid photodamaged hypothesis (Oguchi *et al.* 2011a,b; 2013; Oguchi *et al.* 2009, Schreiber and Klughammer 2013). The hybrid hypothesis proposes that several photo-damaging mechanisms operate in parallel.

For example, if the photosynthetic pigments were the only photosensitizers, the photodamage rates would have been expected to be of the same magnitude for both wavelengths, as the absorption cross section is almost the same. However, this was only the case for the *in vitro* experiments. In turn, if the Mn_4O_5Ca cluster was the main photosensitizer, the observed OJIP curves should have a marked positive band at 300 μs (K-step) as it is seen for Mn-depletion treatments, such as Tris (Strasser 1997, Tóth *et al.* 2011) and heat treatments (Srivastava *et al.* 1997, Tóth *et al.* 2011). Even though the K-step was present in both experimental model systems, the K-step is not dominant under either conditions. The most prominent feature we observed during PSII photodamage *in vivo* was the decrease in JI phase, suggesting that the most affected part during PSII photodamage was linear electron transport. This effect can be explained by direct Mn damage or excessive energy absorbed by photosynthetic pigments.

While the K-step was present in both experimental model systems, it preferentially appeared when the model systems were illuminated at 460 nm. This can be interpreted as happening due to a certain portion of PSII particles suffering damage by direct light absorption by the Mn cluster. This observation agrees with the results of Murphy *et al.* (2017), who reported that blue photons could either induce direct damage to the Mn cluster or cause damage due to excessive excitation. Regardless, the appearance of the K-step occurred faster than the loss of the functional fraction of PSII in both models. For leaves illuminated with 460 nm light, the K-step rate formation was 2.8 times faster than the rate of loss of functional PSII, and for PSII-enriched membranes, the K-step rate was 1.6 times faster than the rate of loss of functional PSII.

All the above can explain why the bleaching effect in blue light was observed, as ROS production seems to be enhanced in blue light. The observed photobleaching *in vivo* could be explained as the effect of low-temperature photodamage (4°C), which may have implications for the mechanism of photodamage (Hendrickson *et al.* 2004). It is known that leaf metabolism is in general lower at low temperatures (Graham and Patterson 1982, Holaday *et al.* 1992). In the case of photosynthesis, all reactions of electron transport (Floyd *et al.* 1971, Fryer *et al.* 1998), oxygen evolution (Brudvig *et al.* 1983, Pastenes and Horton 1996, Hendrickson *et al.* 2004), and the dark phase of photosynthesis (Kobza and Edwards 1987, Holaday *et al.* 1992, Fryer *et al.* 1998) are greatly slowed down at low temperatures. In our experiments done *in vivo*, where the leaves were photodamaged at low temperature, it was expected that the rates of electron transport would be lower. In such a scenario, both the donor and acceptor sides would be limited, which might exacerbate the role of excessive energy absorbed by photosynthetic pigments. In consequence, enhanced production of ROS would be expected, causing the observed photobleaching effect. In fact, it has been reported that at low temperatures the process of photobleaching is markedly enhanced in leaves (Wise and Naylor 1987, Wise 1995). However, none of these findings would explain why photobleaching was stronger under blue light. A feasible explanation of this is the co-occurrence of several blue-absorbing photosensitizers (Mn cluster, chlorophylls or Fe/S centres as mentioned below).

While much attention has been given to the Mn_4O_5Ca cluster as a photosensitiser in the blue, other photosensitisers could operate at the same wavelengths. For example, Kim and Jung (1992, 2001) have proposed Fe/S centres in PSI or in the cytochromes as photosensitizers. While Hideg *et al.* (2000) have demonstrated that singlet oxygen production primarily occurs within PSII, Suh *et al.* (2000, 2002) showed that if cytochrome b_6f is added to PSII particles, photodamage is enhanced. According to Suh *et al.* (2000), the Fe/S centres in the Rieske protein a component of cytochrome b_6f) could be a source of singlet oxygen production. The latter result has been demonstrated further *in vitro* by EPR spectroscopy by Sang *et al.* (2010, 2011a,b). The cytochrome b_6f is present in leaves but not in PSII-enriched membranes, which also would explain the enhanced effect of 460 nm photodamage *in vivo*.

To summarize, the overall mechanisms of PSII photodamage under the present experimental conditions *in vivo* and *in vitro* were similar as both followed single-order kinetics (decrease of the fraction of active PSII, amplitudes of OJIP phases, and presence of the K-step). OJIP analysis indicated that at least two photosensitizers exist: (*1*) photosynthetic pigments; (*2*) a blue photosensitizer, which is likely the Mn cluster (due to K-step formation). The wavelength dependency of PSII photodamage was only relevant *in vivo*, and we propose that the observed differences are mainly due to the presence of multiple photosensitizers and differences in the intra-leaf gradients of light absorption at both wavelengths. Finally, we demonstrated that the penetration depth of the measuring technique is an important factor that affects the results observed in photodamage kinetics.

References

Aro E.M., Virgin I., Andersson B.: Photoinhibition of photosystem II. Inactivation, protein damage and turnover. – BBA-Bioenergetics **1143**: 113-134, 1993.

Becker W., Bergmann A.: Lifetime imaging techniques for optical microscopy. Technical Report. Pp. 41. Becker & Hickl GmbH, Berlin 2003.

Berthold D.A., Babcock G.T., Yocum C.F.: A highly resolved, oxygen-evolving photosystem II preparation from spinach thylakoid membranes: EPR and electron-transport properties. – FEBS Lett. **134**: 231-234, 1981.

Brudvig G.W., Casey J.L., Sauer K.: The effect of temperature on the formation and decay of the multiline EPR signal species associated with photosynthetic oxygen evolution. – BBA-Bioenergetics **723**: 366-371, 1983.

Campbell D.A., Tyystjärvi E.: Parameterization of photosystem II photoinactivation and repair. – BBA-Bioenergetics **1817**: 258-265, 2012.

Evans J.R., Terashima I.: Effects of nitrogen nutrition on electron transport components and photosynthesis in spinach. – Funct. Plant Biol. **14**: 59-68, 1987.

Floyd R.A., Chance B., Devault D.: Low temperature photo-induced reactions in green leaves and chloroplasts. – BBA-Bioenergetics **226**: 103-112, 1971.

Fryer M.J., Andrews J.R., Oxborough K. *et al.*: Relationship between CO_2 assimilation, photosynthetic electron transport, and active O_2 metabolism in leaves of maize in the field during periods of low temperature. – Plant Physiol. **116**: 571-580, 1998.

Graham D., Patterson B.D.: Responses of plants to low, nonfreezing temperatures: proteins, metabolism, and acclimation. – Ann. Rev. Plant Physio. **33**: 347-372, 1982.

Hakala M., Tuominen I., Keränen M. *et al.*: Evidence for the role of the oxygen-evolving manganese complex in photoinhibition of Photosystem II. – BBA-Bioenergetics **1706**: 68-80, 2005.

Havaux M., Strasser R.J., Greppin H.: A theoretical and experimental analysis of the q_P and q_N coefficients of chlorophyll fluorescence quenching and their relation to photochemical and nonphotochemical events. – Photosynth. Res. **27**: 41-55, 1991.

Hendrickson L., Ball M., Wood J. *et al.*: Low temperature effects on photosynthesis and growth of grapevine. – Plant Cell Environ. **27**: 795-809, 2004.

Hideg É., Tamás K., Hideg K., Vass I.: Do oxidative stress conditions impairing photosynthesis in the light manifest as photoinhibition? – Philos. T. Roy. Soc. B **355**: 1511-1516, 2000.

Holaday A.S., Martindale W., Alred R. *et al.*: Changes in activities of enzymes of carbon metabolism in leaves during exposure of plants to low temperature. – Plant Physiol. **98**: 1105-1114, 1992.

Kim C.S., Jung J.: Iron-sulfur centers as endogenous blue light sensitizers in cells: a study with an artificial non-heme iron protein. – Photochem. Photobiol. **56**: 63-68, 1992.

Kobza J., Edwards G.E.: Influences of leaf temperature on photosynthetic carbon metabolism in wheat. – Plant Physiol. **83**: 69-74, 1987.

Laptenok S.P., Borst J.W., Mullen K.M. *et al.*: Global analysis of Förster resonance energy transfer in live cells measured by fluorescence lifetime imaging microscopy exploiting the rise time of acceptor fluorescence. – Phys. Chem. Chem. Phys. **12**: 7593-7602, 2010.

Matsubara S., Chow W.S.: Populations of photoinactivated photosystem II reaction centers characterized by chlorophyll *a* fluorescence lifetime *in vivo*. – P. Natl. Acad. Sci. USA **101**: 18234-18239, 2004.

Melis A.: Photosystem-II damage and repair cycle in chloroplasts: what modulates the rate of photodamage *in vivo*? – Trends Plant Sci. **4**: 130-135, 1999.

Murata N., Takahashi S., Nishiyama Y., Allakhverdiev S.I.: Photoinhibition of photosystem II under environmental stress. – BBA-Bioenergetics **1767**: 414-421, 2007.

Murphy C.D., Roodvoets M.S., Austen E.J. *et al.*: Photoinactivation of photosystem II in *Prochlorococcus* and *Synechococcus*. – PLoS ONE **12**: e0168991, 2017.

Nishiyama Y., Allakhverdiev S.I., Murata N.: A new paradigm for the action of reactive oxygen species in the photoinhibition of photosystem II. – BBA-Bioenergetics **1757**: 742-749, 2006.

Nishiyama Y., Kojima K., Hayashi H. *et al.*: Action of reactive oxygen species in the photoinhibition of photosystem II. – Photosynth. Res. **91**: 284-284, 2007.

Nishiyama Y., Murata N.: Revised scheme for the mechanism of photoinhibition and its application to enhance the abiotic stress tolerance of the photosynthetic machinery. – Appl. Microbiol. Biot. **98**: 8777-8796, 2014.

Oguchi R., Douwstra P., Fujita T. *et al.*: Intra-leaf gradients of photoinhibition induced by different color lights: implications for the dual mechanisms of photoinhibition and for the application of conventional chlorophyll fluorometers. – New Phytol. **191**: 146-159, 2011a.

Oguchi R., Douwstra P., Fujita T. *et al.*: Gradients of photoinhibition in the interior of a leaf induced by photoinhibition lights of different colors. – In: Kuang T., Lu C., Zhang L. (ed.): Photosynthesis Research for Food, Fuel and the Future. Advanced Topics in Science and Technology in China.

Pp. 459-464. Springer, Berlin-Heidelberg, 2013.
Oguchi R., Terashima I., Chow W.S.: The involvement of dual mechanisms of photoinactivation of photosystem II in *Capsicum annuum* L. plants. – Plant Cell Physiol. **50**: 1815-1825, 2009.
Oguchi R., Terashima I., Kou J., Chow W.S.: Operation of dual mechanisms that both lead to photoinactivation of photosystem II in leaves by visible light. – Physiol. Plantarum **142**: 47-55, 2011b.
Ohad I., Adir N., Koike H. *et al*.: Mechanism of photoinhibition *in vivo*. A reversible light-induced conformational change of reaction center II is related to an irreversible modification of the D1 protein. – J. Biol. Chem. **265**: 1972-1979, 1990.
Ohnishi N., Allakhverdiev S.I., Takahashi S. *et al*.: Two-step mechanism of photodamage to photosystem II: step 1 occurs at the oxygen-evolving complex and step 2 occurs at the photochemical reaction center. – Biochemistry-US **44**: 8494-8499, 2005.
Pastenes C., Horton P.: Effect of high temperature on photosynthesis in beans (I. Oxygen evolution and chlorophyll fluorescence). – Plant Physiol. **112**: 1245-1251, 1996.
Porra R.J., Thompson W.A., Kriedemann P.E.: Determination of accurate extinction coefficients and simultaneous equations for assaying chlorophylls *a* and *b* extracted with four different solvents: verification of the concentration of chlorophyll standards by atomic absorption spectroscopy. – BBA-Bioenergetics **975**: 384-394, 1989.
Sang M., Ma F., Xie J. *et al*.: High-light induced singlet oxygen formation in cytochrome b_6f complex from *Bryopsis corticulans* as detected by EPR spectroscopy. – Biophys. Chem. **146**: 7-12, 2010.
Sang M., Qin X.-C., Wang W.-D. *et al*.: High-light induced superoxide anion radical formation in cytochrome b_6f complex from spinach as detected by EPR spectroscopy. – Photosynthetica **49**: 48-54, 2011a.
Sang M., Xie J., Qin X.-C. *et al*.: High-light induced superoxide radical formation in cytochrome b_6f complex from *Bryopsis corticulans* as detected by EPR spectroscopy. – J. Photoch. Photobio. B **102**: 177-181, 2011b.
Schreiber U., Klughammer C.: Wavelength-dependent photodamage to *Chlorella* investigated with a new type of multicolor PAM chlorophyll fluorometer. – Photosynth. Res. **114**: 165-177, 2013.
Srivastava A., Guissé B., Greppin H., Strasser R.J.: Regulation of antenna structure and electron transport in photosystem II of *Pisum sativum* under elevated temperature probed by the fast polyphasic chlorophyll *a* fluorescence transient: OKJIP. – BBA-Bioenergetics **1320**: 95-106, 1997.
Strasser B.J.: Donor side capacity of photosystem II probed by chlorophyll *a* fluorescence transients. – Photosynth. Res. **52**: 147-155, 1997.
Strasser R.J., Tsimilli-Michael M., Qiang S., Goltsev V.: Simultaneous *in vivo* recording of prompt and delayed fluorescence and 820-nm reflection changes during drying and after rehydration of the resurrection plant *Haberlea rhodopensis*. – BBA-Bioenergetics **1797**: 1313-1326, 2010.
Suh H.J., Kim C.S., Jung J.: Cytochrome b_6f complex as an indigenous photodynamic generator of singlet oxygen in thylakoid membranes. – Photochem. Photobiol. **71**: 103-109, 2000.
Suh H.J., Kim C.S., Lee J.Y., Jung J.: Photodynamic effect of iron excess on photosystem II function in pea plants. – Photochem. Photobiol. **75**: 513-518, 2002.
Takahashi S., Badger M.R.: Photoprotection in plants: a new light on photosystem II damage. – Trends Plant Sci. **16**: 53-60, 2011.
Takahashi S., Milward S.E., Yamori W. *et al*.: The solar action spectrum of photosystem II damage. – Plant Physiol. **153**: 988-993, 2010.
Takahashi S., Murata N.: How do environmental stresses accelerate photoinhibition? – Trends Plant Sci. **13**: 178-182, 2008.
Tóth S.Z., Nagy V., Puthur J.T. *et al*.: The physiological role of ascorbate as photosystem II electron donor: protection against photoinactivation in heat-stressed leaves. – Plant Physiol. **156**: 382-392, 2011.
Tyystjärvi E.: Photoinhibition of Photosystem II and photodamage of the oxygen evolving manganese cluster. – Coordin. Chem. Rev. **252**: 361-376, 2008.
Tyystjärvi E.: Photoinhibition of Photosystem II. – Int. Rev. Cel. Mol. Bio. **300**: 243-303, 2013.
Tyystjärvi E., Aro E.M.: The rate constant of photoinhibition, measured in lincomycin-treated leaves, is directly proportional to light intensity. – P. Natl. Acad. Sci. USA **93**: 2213-2218, 1996.
van Gorkom H.J., Schelvis J.P.M.: Kok's oxygen clock: what makes it tick? The structure of P680 and consequences of its oxidizing power. – Photosynth. Res. **38**: 297-301, 1993.
Vass I.: Role of charge recombination processes in photodamage and photoprotection of the photosystem II complex. – Physiol. Plantarum **142**: 6-16, 2011.
Vass I.: Molecular mechanisms of photodamage in the Photosystem II complex. – BBA-Bioenergetics **1817**: 209-217, 2012.
Vavilin D.V., Tyystjärvi E., Aro E.M.: In search of a reversible stage of photoinhibition in a higher plant: No changes in the amount of functional Photosystem II accompany relaxation of variable fluorescence after exposure of lincomycin-treated *Cucurbita pepo* leaves to high light. – Photosynth. Res. **45**: 239-247, 1995.
Verhoeven A.: Sustained energy dissipation in winter evergreens. – New Phytol. **201**: 57-65, 2014.
Wise R.R.: Chilling-enhanced photooxidation: The production, action and study of reactive oxygen species produced during chilling in the light. – Photosynth. Res. **45**: 79-97, 1995.
Wise R.R., Naylor A.W.: Chilling-enhanced photooxidation evidence for the role of singlet oxygen and superoxide in the breakdown of pigments and endogenous antioxidants. – Plant Physiol. **83**: 278-282, 1987.
Zavafer A., Cheah M.H., Hillier W. *et al*.: Photodamage to the oxygen evolving complex of photosystem II by visible light. – Sci. Rep-UK **5**: 16363, 2015b.
Zavafer A., Chow W.S., Cheah M.H.: The action spectrum of Photosystem II photoinactivation in visible light. – J. Photoch. Photobio B. **152**: 247-260, 2015a.
Zavafer A., Koinuma W., Chow W.S. *et al*.: Mechanism of photodamage of the oxygen evolving Mn cluster of photosystem II by excessive light energy. – Sci Rep-UK **7**: 7604, 2017.